Resuspension of Threat Agents from Paved Surfaces and Recommended Resuspension Factors — Field Experiments with Pedestrian or Personnel Activity and Vehicles

Michael D.R. Kaminski,[1] Nico Daiyega,[1] and Hannah Jaglinski[1,2]

Abstract—**Resuspension of hazardous particles from paved surfaces poses significant risks during radiological contamination scenarios. Accurate modeling of particle resuspension dynamics is essential for developing effective mitigation strategies and ensuring public and responder safety. However, default resuspension factors in models may underestimate risks, particularly during emergency operations involving pedestrian and vehicle activity on freshly contaminated surfaces.**

To address these gaps, we conducted pilot-scale field experiments using Arizona Test Dust (ATD) as a surrogate for threat agents. Human activities included casual walking, vigorous walking (marching), and vacuuming on concrete surfaces, while vehicle tests involved driving a sport utility vehicle (SUV) over asphalt in both drive-through (tires passing over dust) and drive-over (undercarriage passing over dust) configurations. Resuspension factors (S_f) were calculated for particle size ranges from 0.5–10 µm. Casual walking produced low resuspension factors, from <10^{-5} m^{-1} for 0.5-1.0 µm particles to <3×10^{-3} m^{-1} for 5-10 µm particles. In contrast, marching, which served as a surrogate for vigorous pedestrian or personnel movement, substantially increased resuspension, with S_f values ranging from 2×10^{-5} m^{-1} at 0.1-1 µm to 2×10^{-3} m^{-1} for 5-10 µm particles. Vacuuming caused measurable resuspension for smaller particles ($S_f = 1.4\times10^{-3}$ m^{-1}), while larger particles remained undetectable. Vehicle tests showed higher resuspension factors for larger particles, with S_f values ranging from 3×10^{-4} m^{-1} to 2×10^{-2} m^{-1} during the first pass. Subsequent passes eventually reduced resuspension factors by an order of magnitude. These findings reveal significantly higher resuspension during emergency operations than many models assume. Our results apply to scenarios involving radioactive fallout, chemical, and biological agents, offering critical data to improve contamination control, emergency response planning, and risk assessment models.
Health Phys. XXX(00):00–00; 2026

Keywords: exposure; population; radiation; airborne

[1]Strategic Security Sciences Division, Argonne National Laboratory, IL; [2]DePaul University, IL.

For correspondence contact: Michael D.R. Kaminski, 9700 S. Cass Ave, Lemont, IL 60441, or email: **kaminski@anl.gov**.

Supplemental digital content is available in the HTML and PDF versions of this article on the journal's website (www.health-physics.com).

(Manuscript accepted 18 May 2026)
0017-9078/XXX/00

DOI: 10.1097/HP.0000000000002195

INTRODUCTION

Resuspension of hazardous particles from paved surfaces poses significant risks during chemical, radiological, and biological contamination scenarios. These particles, once airborne, can be inhaled by emergency responders and the public, increasing exposure risks and complicating mitigation efforts. Accurate modeling of resuspension dynamics is essential for developing effective contamination control strategies, informing emergency response protocols, and ensuring public safety. In particular, existing radiation dose and plume models do not provide sufficient guidance on appropriate resuspension factors S_f, defined as the concentration of threat agent in the air divided by the areal concentration on the ground, aside from default values (10^{-6}-10^{-5} m^{-1}) that may underestimate the risks associated with emergency operations involving pedestrian or personnel and vehicle activity on freshly contaminated surfaces.

While previous studies have explored resuspension mechanisms, most have focused on indoor environments or outdoor air pollution unrelated to emergency contamination scenarios. Few studies have investigated resuspension factors for radioactive fallout or other threat agents under conditions relevant to emergency response, such as vigorous pedestrian activity or vehicle movement on paved surfaces. This lack of data hinders the ability of modelers to accurately assess risks and make informed decisions regarding personal protective equipment (PPE), operational stay times, and evacuation vs. shelter-in-place strategies.

To address these gaps, we conducted pilot-scale field experiments to measure resuspension factors for activities likely to occur during the emergency phase following the deposition of threat agents onto paved surfaces. While the properties of particulate forms of threat agent can vary, we chose to employ Arizona Test Dust (ATD) as a surrogate for radioactive fallout (Glasstone and Phillips 1977; Crocker et al. 1966; Harper et al. 2007) and other threat agents given its similar properties (Owens and Walling 1996; Pires et al. 1994; Thorpe and Harrison 2008) and evaluated its resuspension during casual walking, vigorous activity (marching), vacuuming, and vehicle driving.

Resuspension factors S_f from casual walking was low and similar to limited prior studies with values <10^{-5} m^{-1}. Marching, an approach chosen to replicate the increased intensity and pace of movement typically observed during emergency evacuations, as opposed to regular walking, resulted in resuspension factors that increased with increasing size of particle with average values of 2×10^{-5} m^{-1}at 0.1-1 μm to 2×10^{-3} m^{-1} for 5-10 μm particles. Vacuuming produced measurable dust air concentrations at 0.5-1 μm with $S_f = 1.4 \times 10^{-5}$ with larger-sized particles below detection limits.

Driving a large sports utility vehicle (SUV) over road dust produced similar resuspension factors whether the tires drove over the dust or if the undercarriage was driven over the dust. As with marching, larger particles had larger resuspension factors. Adjusting for complete coverage of the road surface, S_f increased from 3×10^{-4} m^{-1} for 0.5-1.0 μm particles to 2×10^{-2} m^{-1} for 5-10 μm particles for the first pass of the vehicle over the dust. After the 6th pass of the vehicle, S_f decreased by an order of magnitude but was still substantially higher than default model values — 6×10^{-5} m^{-1} for 0.5-1.0 μm particles to 2×10^{-3} m^{-1} for 5-10 μm particles.

These experiments provide critical data for improving contamination control, emergency response planning, and risk assessment models, with applications to radiological, chemical, and biological threat agents.

MATERIALS AND METHODS

Surrogate dust and measurement instruments

Arizona Test Dust (ATD, A1 Ultrafine Test Dust, density = 2.5-2.7 g cm^{-3}, Particle Technology, Inc, Arden Hills, MN) was kept at ambient laboratory conditions (20°C and ~60% RH) prior to laboratory and field tests. No additional measures were taken to control the humidity of the samples during field trials. This ATD was chosen to mimic the properties of radioactively contaminated environmental dust, consistent with cesium contaminated urban dust from Fukushima and Goiania (Tang et al. 2022). We utilized a range of aerosol measurement instruments — the Aerodynamic Particle Sizer APS 3321 and four Optical Particle Counters (OPC; Model 3330) were from TSI Inc. (Shoreview, MN), and a Plantower PMS 5003 particle counter (Plantower Technology, Nanchang, China) was modified to provide real-time data reporting and is referred to as a "custom particle counter" (CPC) hereafter. These instruments collectively measure particulate matter concentrations and particle size distributions in the air. A Kestrel anenometer (Kestrel Instruments, Model 3000, Boothwyn, PA) gathered real-time wind speed, air temperature, and relative humidity.

Calibration of measurement instruments

A plexiglass box (46.8L × 48.1W × 20.5H cm^3 = 0.046 m^3) was used to contain an aerosol of particles generated by pressurized air. To test the relative response of each of the aerosol measurement instruments, an amount of ATD (1, 3, 10, 25, 50, 100, or 250 mg) was placed in the middle of the test stand (7.6-cm cube) held near the middle of the test chamber. We used an anti-static gun multiple times to eliminate static from the particles inside the bottle and on the stand (Milty Pro Zerostat 3, Fisher Scientific, Waltham, MA). An air hose was fitted with a knife edge and pointed toward the center of the test stand. The inlet hoses for the APS 3321 and the OPC devices were collocated in a corner opposite to the direction of the pressurized air from the air hose over the test stand that held varying amounts of ATD. The devices were turned on for 30 s of background collection before the forced air (31 m s^{-1}) was turned on for 10 s. Then, the pressurized air was turned off. Collection continued for another ~140 s. This was repeated in triplicate for each mass of ATD. The calculated dust concentrations inside the box corresponded to 22 mg m^{-3} – 5,400 mg m^{-3}. The relative response of each of the devices was benchmarked against the response from the APS 3321, which served as the gold standard, to produce relative calibration factors for field trials in order to compute resuspension factors S_f defined as:

$$S_f = \frac{\text{particle concentration in the air } (\#/\text{m}^3)}{\text{particle concentration on the ground } (\#/\text{m}^2)} = \frac{C_{PM}}{\left(\frac{N_p}{A_p}\right)}, \quad (1)$$

where C_{PM} is the adjusted particle concentrations from the various aerosol measurement devices, N_p is number of particles on the ground, and A_p is the area covered in ATD (see Supplemental S1, *https://links.lww.com/HP/A354*).

Human activity tests

Casual walking. A sealed concrete floor was prepared by mopping with a dilute cleaner and water. A tent enclosure (see Fig. 1, 1.25 m wide × 5.28 m long × 2.31 m tall) was erected over the floor to create a controlled environment. Aerosol measurement devices were positioned at the center, entrance, and back of the tent, with intake hoses placed at a height of 1 m. The height of 1 m was chosen in accordance with US EPA (US EPA 2017) and US DOE guidance (Nielsen and Fournier 2025) and generally represents the breathing height of a child and provides conservative values for resuspension.

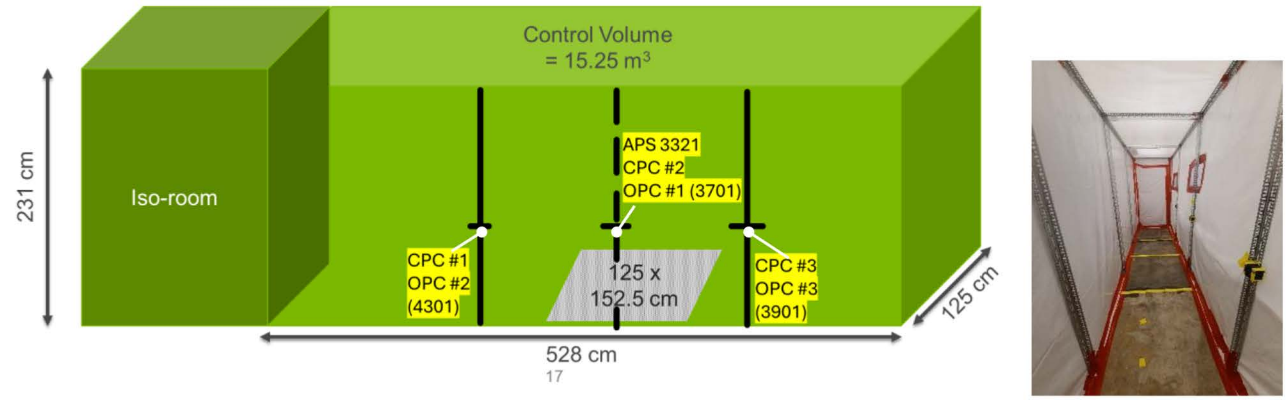

Fig. 1. Human activity tent showing the locations of the colocated aerosol measurement devices. The photo (right) shows the inside of the tent taken from the iso-room.

In preliminary tests, we observed that high concentrations of ATD would be needed to produce a measurable signal. To obtain a measurable signal, we spread 82.9 g ATD over the entire tent footprint (6.6 m^2, dust loading = 12.6 g m^{-2}). To do this, ATD was added to a #200 stainless steel sieve (ASTM Standard Testing Sieve, VWR Scientific, West Chester, PA) and held about 0.3 m above the ground and the side of the sieve hit by hand to shake powder through the sieve onto the ground. Any areas that appeared to have uneven coverage were brushed over gently with a flat plastic blade. Then, the participant walked at a normal pace back and forth the entire length of the tent for a duration of ~15 s. We noted that humidity increased rapidly due to perspiration by the participant and this may have depressed resuspension of material. Then, the participant repeated the walking as before for a duration of ~15 s.

Marching. After the casual walking tests, the air was allowed to settle for 10's of minutes. No additional dust was added to the ground. Then, aggressive marching tests were initiated. Marching involved raising each knee until the thigh was nearly horizontal to the floor while moving randomly over a 125 cm × 152.5 cm area in the tent for 35 s. Aerosol concentrations were recorded by collocated APS and OPC devices, adjusted using calibration factors, and averaged to compute resuspension factors (see Supplemental S2, *https://links.lww.com/HP/A354*). Humidity was still problematic, but the marching created much more disruption of dust on the floor.

Vacuuming. Following marching activities, the air was allowed to settle for 10's of minutes. A vacuum cleaner (Euroclean GD-930-H, Plymouth, MN) was used to clean the tent floor with a standard floor vacuum head (27 cm long). Air concentrations were recorded using the APS, as larger particle sizes were below detection limits for the OPC devices.

Vehicle driving tests

Control tests. Background tests were conducted in an open garage (19.5' × 25', T = 65°F, RH=85%) to ensure no particles were emitted by the vehicle exhaust. The SUV (2003 Chevrolet Trailblazer EXT, 4WD, 4.2L) was positioned in the garage, and no elevated air particulate concentrations for particles >0.3 µm were measured before and after starting the engine and revving to 2,000 RPM.

Drive-through and drive-over tests. Vehicle tests were conducted outside on a roadway at the research campus (6.4 m wide, 350 m long). A test patch (6.4 m wide × 10 m long) was recoated with liquid pavement sealer (S1010 MasterSeal Pavement Sealer, SealMaster Products and Equipment, Alsip, IL) and allowed to cure for 30 d. ATD was dispensed onto the test patch using a flour sifter (drive-through tests, 1 m long, 0.3 m wide, track width = 1.62 m, dust load = 20.4 g m^{-2}, Fig 2) or a #200 stainless steel sieve (drive-over tests, 2 m long × 0.3 m wide, dust load = 10.2 g m^{-2}), followed by gentle brushing to ensure uniform coverage. The SUV (SUV, 2003 Chevrolet Trailblazer EXT, 4WD 4.2L, Dextero DHT2 front tires, Linglong Crosswind H/T rear tires, P245/65R17, 20.3 cm undercarriage ground clearance, 2,253 kg curb weight) was driven over the test patch at 64 km h^{-1} (40 mph, speed confirmed with cell phone GPS and the vehicle speedometer) multiple times, with aerosol measurement devices positioned at the center and corners of the test patch at a height of 1 m (Fig 3). Air concentrations were recorded and adjusted using calibration factors to compute resuspension factors (see Supplemental S2, *https://links.lww.com/HP/A354*).

Short sections of dust were employed to limit the amount of dust released to the environment and to ensure airborne dust concentrations were within the linear range of our aerosol measurement instruments.

In preliminary tests, the SUV driven at 30-40 mph caused a small, but measurable concentration of resuspended

Fig. 2. Photo of the ATD seeded with a flour-sifter onto the test area prior to trials. The seeded area corresponds to the track width of the tires (1.62 m).

natural road dust in the 0.5-2.5 μm size ranges. This natural dust was eliminated by cleaning the test patch prior to driving tests by using a leaf blower (Kobalt KHB 20248-03, 14.1 m^3 min^{-1}, Homer, IL) held at 10-20 cm above the ground at an angle and blowing from west to east in the direction of the prevailing wind across the test patch. Then the test patch was vacuumed using a flat, floor nozzle attachment (Milwaukee M18 Fuel 3-in-1 Backpack Vacuum, 25 cm long nozzle). The wind was calm (1.3 m s^{-1} average, 1.8 m s^{-1} maximum), the relative humidity was 55% and the air and ground temperatures were 63-65° F and 58°F, respectively.

RESULTS

Particulate monitoring benchmarking

Aerosol measurement devices differ in their measurement principles, applications, and technical specifications. To compare the responses, we collected ATD aerosol concentrations with the devices collocated within the Plexi-glass box enclosure. The linearity of all devices were very good for the expected particle air concentration range (Fig. 4) of <<500 raw counts per cm^3 of air. Then by computing the ratio of the signal strength of each sensor (Table 1, converted into # of particles per cm^3 of air), we obtained relative calibration factors against the APS 3321. The resulting relative calibration factors carried satisfactory uncertainties (Table 2) and were used to convert particle air concentrations for each size range recorded by one particular device into values comparable with the APS 3321.

Walking and marching tests

Casual walking failed to produce a measurable concentration of dust in the air in any of the monitors located inside the tent (Fig. 5). Resuspension factor detection limits (Table 3) ranged from $<1 \times 10^{-5}$ m^{-1} for 0.5-1.0 μm

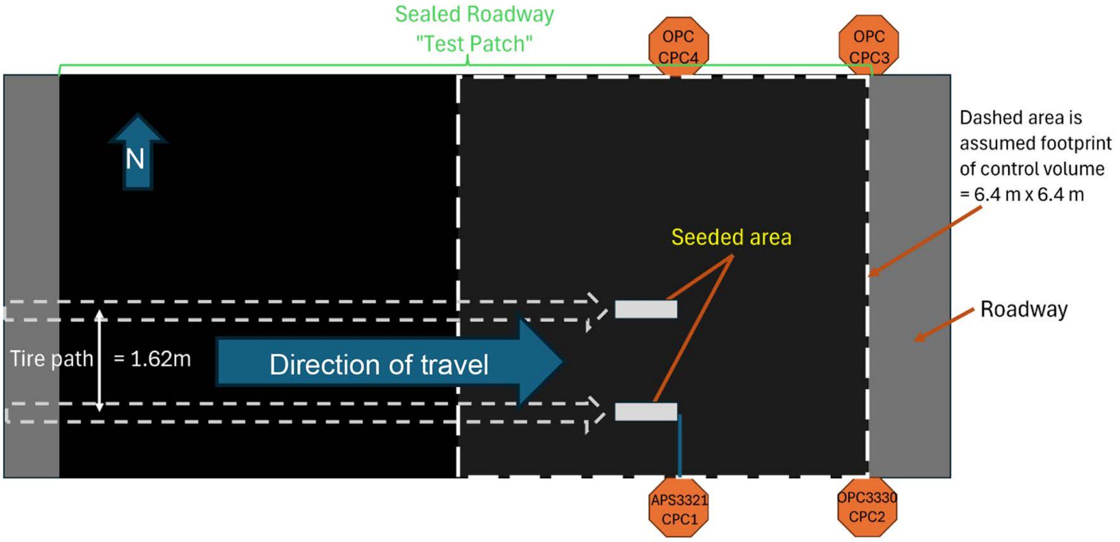

Fig. 3. Drawing of the vehicle test area. The SUV traveled from left-to-right nearest the poles that held the APS/CPC1 and OPC3300/CPC2 (see Supplemental S3, *https://links.lww.com/HP/A354*).

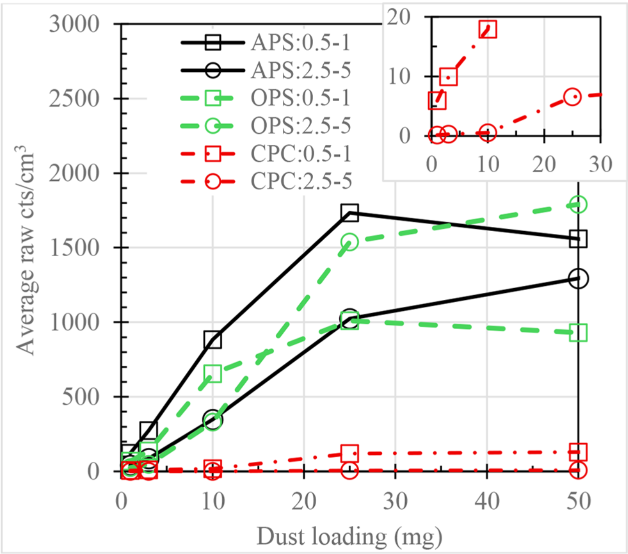

Fig. 4. Linearity of the various devices to ATD particle air concentrations (0.5-1 μm and 2.5-5 μm). The other size ranges are not displayed but show similar trends. Note that the CPC has poor sensitivity compared to the APS and OPC and especially to particles >2.5 μm (see inset).

Table 1. Example of raw counts (particles cm^{-3}) for the APS, OPC and CPC devices for a single 3 mg ATD dispersion tests.

PM	Particle size range			
device	0.5-1 μm	1-2.5 μm	2.5-5 μm	5.0-10 μm
CPC	5.4	0.9	0.1	0.1
APS	156	109	34.5	1.7
OPC	60.2	47	17.1	2.5

particles and progressively increased to <3×10^{-3} m^{-1} for 5.0-10 μm.

Marching generated measurable airborne dust concentrations across all particle size ranges (Fig. 5). The S_f increased with particle size, consistent with prior literature. Peak S_f ranged from 2×10^{-4} m^{-1} for 1.0-2.5 μm particles to 4×10^{-3} m^{-1} for 5-10 μm particles (Table 4). Measurable airborne dust was detected approximately 7 s after the onset of marching, which we infer reflects the time required for marching-induced turbulence to entrain and maintain the test dust in suspension. Dust was also detected downstream throughout the tent: the "Marching, downstream" plot showed airborne particles of all sizes >0.5 μm and 1.3 m from the marching area starting approximately 20 s after marching ended (Fig. 5), confirming that dust was resuspended and transported in air. Collectively, these findings indicate that marching is a more suitable surrogate for scenarios involving dense, vigorous pedestrian or personnel movement — such as mass evacuation on foot or rapid first-responder activity — than for a single individual walking quickly. Nevertheless, the steady-state airborne concentrations reflected by the resuspension factors in Table 4 are likely most representative of conditions within or close to the active movement zone, rather than at greater distances where concentrations would be expected to attenuate.

Comparing the walking and marching results to the literature is difficult because of a dearth of studies that account for concrete or asphalt pavement. Walking on a granolithic concrete floor in a laboratory changing room, S_f=3×10^{-3} to 10^{-4} m^{-1} was reported with plutonium contamination (Brunskill 1967). More recently, a person marching in a pattern on a concrete pad inside a test chamber contaminated with CeO_2 produced S_f in the range of 2-6×10^{-6} m^{-1} (Glen and Pennington 2020). Other studies of relevance report S_f spanning orders of magnitude making correlation difficult. On linoleum, using a "more vigorous walking pace" (up to 200 steps/min) and plutonium nitrate/oxide, S_f =2×10^{-5} – 10^{-4} m^{-1} was measured (Jones and Pond 1967). Similarly, walking upon vinyl floors resuspended spores with a S_f=1.8×10^{-5} m^{-1} (Buttner et al. 2002) to 3.5×10^{-3} m^{-1} (Hambraeus et al. 1978) while S_f=4.5×10^{-2} m^{-1} for ambient dust (Shouaghnessy and Vu 2012), although the particles used in these studies are significantly less dense than the plutonium and ATD in our study. Much higher values were measured by Lai et al. (2017), where walking at 40 steps/min produced ultrafine test dust air concentration sufficient for S_f=1.2×10^{-3} m^{-1} for 0.9 μm particles and 1.2×10^{-1} m^{-1} for larger 9 μm size particles.

Vacuuming tests

Vacuuming the dusty floor produced a measurable amount of aerosol in only the 0.5-1.0 μm size fraction with S_f=1.4×10^{-5} m^{-1} (Table 3). The larger sizes were not detected above limits with detection limits steadily increasing with size. The S_f value for 0.5-1.0 μm is

Table 2. Calculated relative calibration factors for settling periods based on triplicate runs of 3 mg ATD dispersion tests.

PM	Particle size range and standard error							
device	0.5-1 μm	±	1-2.5 μm	±	2.5-5 μm	±	5.0-10 μm	±
APS/APS	1	0	1	0	1	0	1	0
APS/CPC	25	5	97	28	267	94	23	9
OPC/CPC	12	1	52	4.9	155	26	36	11
APS/OPC	2.1	0.5	1.8	0.4	1.7	0.3	0.6	0.1

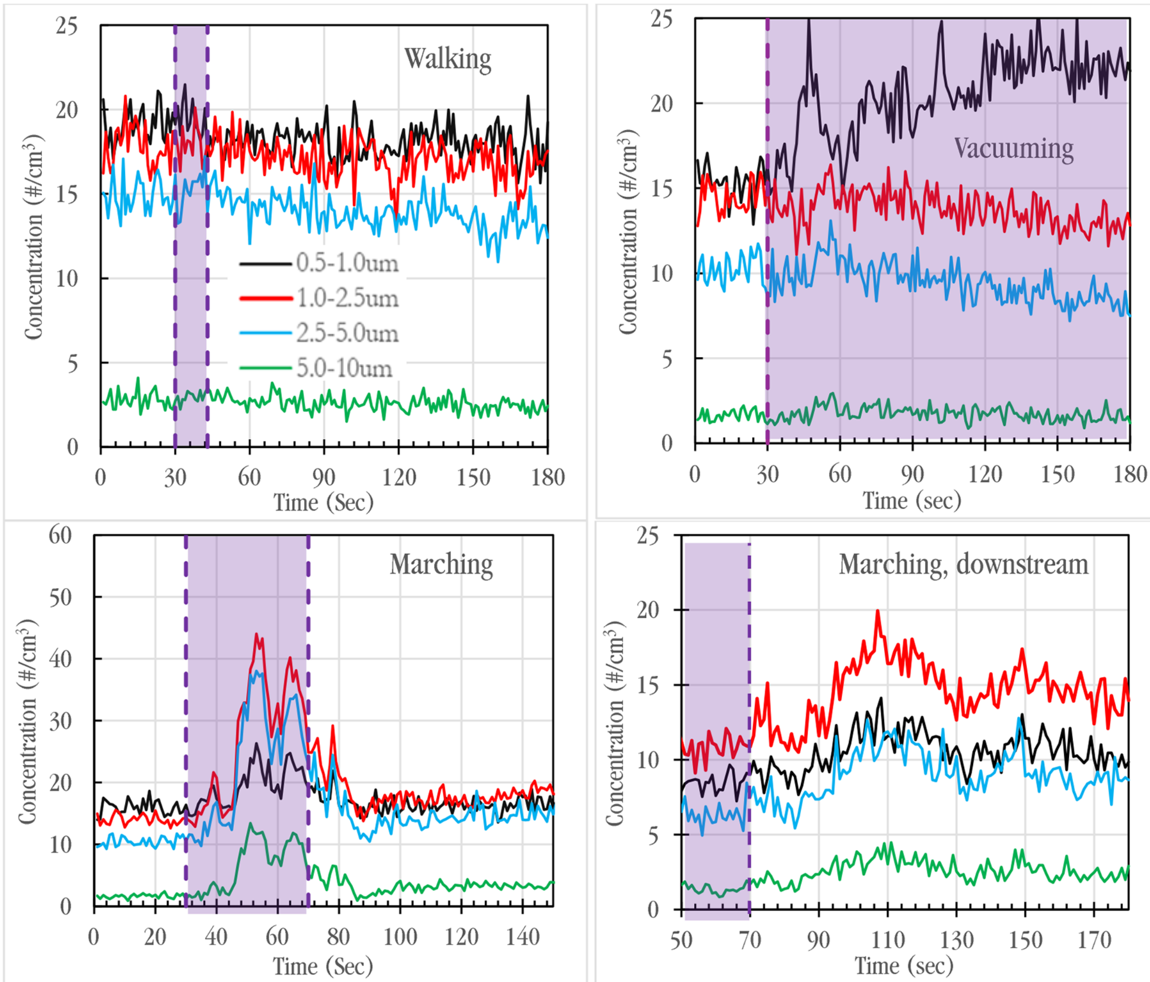

Fig. 5. Aerosol measurements for casual walking (upper left), vacuuming (upper right), and marching activities (bottom left and right). The purple shaded area indicates the duration of that activity. The bottom, right graph (Marching, downstream) shows the measurement at the end of the tent showing the time delay before the plume of dust reached that detector.

consistent with vacuum cleaning with a HEPA-filtered upright cleaner over sieved house dust on hardwood laminate flooring (<300 μm, dust loading = 1 g m^{-2}) (Lewis et al. 2018, Figs. 4-6 therein) that produced size dependent S_f of 1.5×10^{-5} m^{-1}, 5.1×10^{-5} m^{-1}, 4.7×10^{-5} m^{-1} for 2.5, 5.0, and 10 μm, respectively (see Supplemental S4, *https://links.lww.com/HP/A354*). Other studies on hard surfaces like pavement could not be found but the trend for carpeted surfaces indicates that resuspension increases with particle size (Corsi et al. 2008; Ferro et al. 2004; Ji 2020).

Table 3. Resuspension factors (m^{-1}) measured during walking and marching tests.

Particle size (μm)	Walking	Vacuuming
0.5-1.0	$<1 \times 10^{-5}$	1.4×10^{-5}
1.0-2.5	$<3 \times 10^{-5}$	$<2 \times 10^{-5}$
2.5-5.0	$<2 \times 10^{-4}$	$<2 \times 10^{-4}$
5.0-10.0	$<3 \times 10^{-3}$	$<3 \times 10^{-3}$

Vehicle testing

Drive-through tests. ATD was seeded on a test patch such that the tires would pass directly over the test patch of dust. This was done to purposely discriminate the difference between resuspension caused by the tires and resuspension caused by the draft of air (see "Vehicle drive-over" below) created by the fast moving vehicle.

The resuspension of dust was substantial each time the tires passed through the dust at 64 km h^{-1} (40 mph, see Fig. 6). Each pass produced a measurable plume of the ATD in the air (Fig. 7 and Supplemental S5, *https://links.lww.com/HP/A354*) and these produced peak and average resuspension factors (Fig. 8) that increased with increasing particle size. For example, the peak S_f was

Table 4. Measured particle air concentrations and calculated resuspension factors for the collocated APS and OPC at the center of the tent during marching activities.

	Measured air concentration (particles cm^{-3})				Calculated resuspension factors S_f (m^{-1})			
	Peak value		Average value		Peak values		Average values	
Size (μm)	APS	OPC	APS	OPC	S_f	±	S_f	±
0.5-1.0	10.4	21.3	3.2	7.2	6×10^{-5}	3×10^{-5}	2×10^{-5}	1×10^{-5}
1.0-2.5	29.9	30.7	11.8	12.2	2×10^{-4}	4×10^{-6}	9×10^{-5}	2×10^{-6}
2.5-5.0	27.7	22.4	11.6	8.3	2×10^{-3}	2×10^{-4}	7×10^{-4}	2×10^{-4}
5.0-10.0	11.9	4.86	4.5	1.8	6×10^{-3}	4×10^{-3}	2×10^{-3}	1.5×10^{-3}

1.5×10^{-4} m^{-1} for 1.0-2.5 μm, 1×10^{-3} m^{-1} for 2.5-5 μm, and 5×10^{-3} m^{-1} for 5-10 μm particles for the first vehicle pass. The first three passes produced similar S_f, while passes 4-6 were measurably lower. After six passes the S_f was reduced by an order of magnitude from the first pass with an $S_f = 1\times10^{-5}$ m^{-1} for 1.0-2.5 μm, 1×10^{-4} m^{-1} for 2.5-5 μm, and 3×10^{-4} m^{-1} for 5-10 μm particles.

It is important to note that the calculation of the resuspension carries additional uncertainties. If the amount of dust removed from the original test patch is small, then no corrections have to be made for the dust loading term — the denominator in eqn (1). However, if the amount of dust removed is substantial, then the number of particles on the ground N_p would need to be reduced in calculating S_f after each vehicle pass to account for the lower dust loading. The result is a proportional increase in the value of S_f if the air concentration generated by that particular vehicle pass C_{PM} does not change substantially. For example, each pass of the vehicle removed a significant fraction of 5-10 μm particles (Fig. 8, right side). The first three passes removed 0.3, 0.3, and 0.5 of the calculated initial dust loading. Thus, the S_f should be adjusted to account for the new dust loading after each vehicle pass. However, these fractions have obvious problems since they total more than 1.0. But it is clear from our field tests that the dust removed from the test patch also redeposited onto the ground ahead of the test patch. Therefore, this newly deposited dust must have contributed to the subsequent air concentration generated in the next vehicle pass and the effective area of the test patch A_p is larger. Mathematically, the overall results is that N_p is smaller after each vehicle pass but A_p is larger, and the two values offset to some degree. With each pass, the exact value of N_p and A_p become more uncertain but, since they offset, we chose to ignore this effect and recognize that it adds an estimated uncertainty of a factor of 2-5 on our reported values in Fig. 8.

Notwithstanding, the trends in Fig. 8 are consistent with the literature. Nicholson and Branson (1990) performed drive over tests very similar to ours at 64 km h^{-1} and found that the resuspension of particles was also significant with 24-59% of particles originally on the pavement removed with a single pass of a medium sized car. There was a general increase in the amount of dust resuspended with increasing size of the particles with estimated S_f for the first pass of the vehicle of 1.2×10^{-1} m^{-1}, 2.4×10^{-2} m^{-1}, and 2.9×10^{-1} m^{-1} for 4.2, 9.5, and 12 μm particles, respectively (see Supplemental S6, *https://links.lww.com/HP/A354*). In those tests, most of the silica dust (1 g cm^{-3}) was removed from the surface after two vehicle passes. The smallest particles were slightly more difficult to resuspend (4.2 μm) with 55% of silica dust removed after 10 passes compared to 62% for 9.5 μm and 73% for 12 μm particles. Interestingly, he measured significant fractions of all particles resuspended, 20-30%, even at speeds as low as 8 and 16 km h^{-1} (5 and 10 mph). Sehmel (1973) reported lower but substantial fractions of 8 μm (mean diameter) zinc sulfide particles resuspended from truck drive-through tests on asphalt of 0.25% and 0.67% for 8 and 80 km h^{-1} (5 and 50 mph), respectively.

Vehicle drive-over tests. The vehicle driver-over tests were qualitative due to the extremely high background of particulate in the air during trials. However, the qualitative results provided valuable and actionable information. Each overpass over the ATD clearly removed a significant fraction of the dust into the air. When viewing the video of the vehicle passing over the ATD, one can clearly see the dust mixing with the air in an upward direction and not simply transferred a short distance along the pavement (Fig. 9). Before and after pictures (Fig. 10) of the remaining ATD on the pavement was qualitatively similar to the pass-through tests suggesting similar resuspension factors are appropriate.

This observation is supported further by the results of Nicholson et al. (1989). Compared to his drive through tests, there was very little difference in the amount of dust remaining on the pavement with each vehicle pass, in agreement with our results. For example, the mid-sized car removed 20% of 4.2 μm, 50% of 9.5 μm, and 69% of 12 μm particles after a single pass at 64 km h^{-1}.

Although a different scheme, Sehmel (1973) passed a truck next to the lane containing contaminated dust. At 80 km h^{-1} (50 mph), Sehmel reported a small fraction

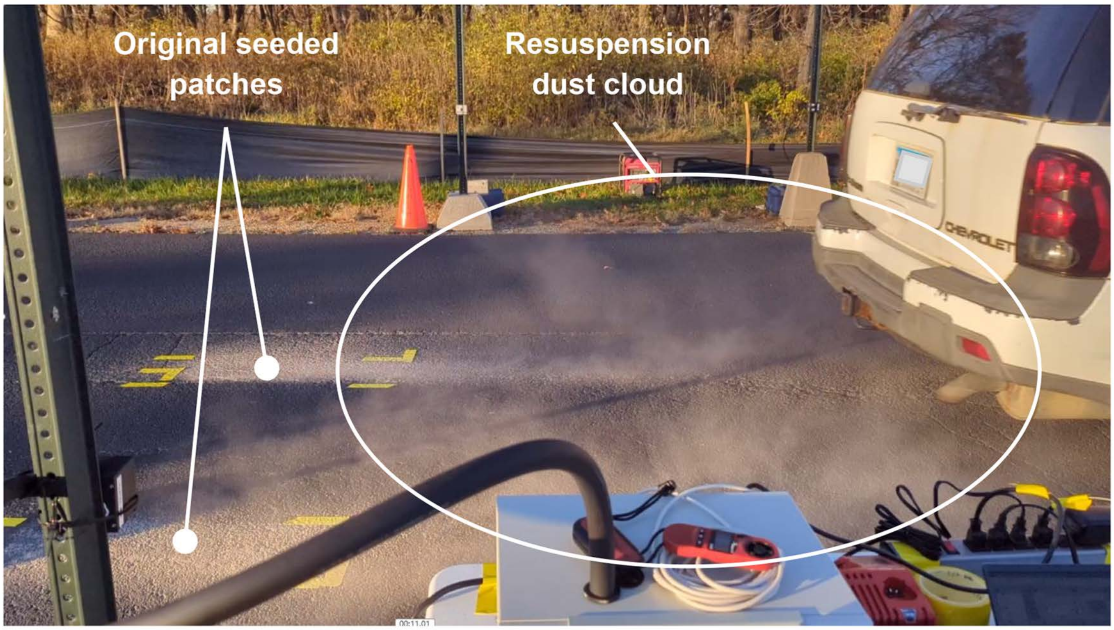

Fig. 6. Picture of SUV passing through the test patch and the dust cloud created by the tires and the wake of the vehicle.

of dust resuspended, 6.7×10^{-3} resuspended per pass, measuring an order of magnitude smaller than when he passed the truck through the contaminated lane. Thus, one may conclude that resuspension due to the draft turbulence created by driving over a dusted area is approximately equal to the resuspension created by driving the tires directly over the dust. Moreover, the resuspension due to the draft created by driving next to a contaminated lane is an order of magnitude smaller than the turbulence created by driving over a contaminated lane. In addition, resuspension caused by a passenger car was an order of magnitude smaller than that of a pickup truck (Sehmel 1973). Glen and Pennington (2020) reported maximum resuspension factors of 4.6×10^{-5} m^{-1} for 10

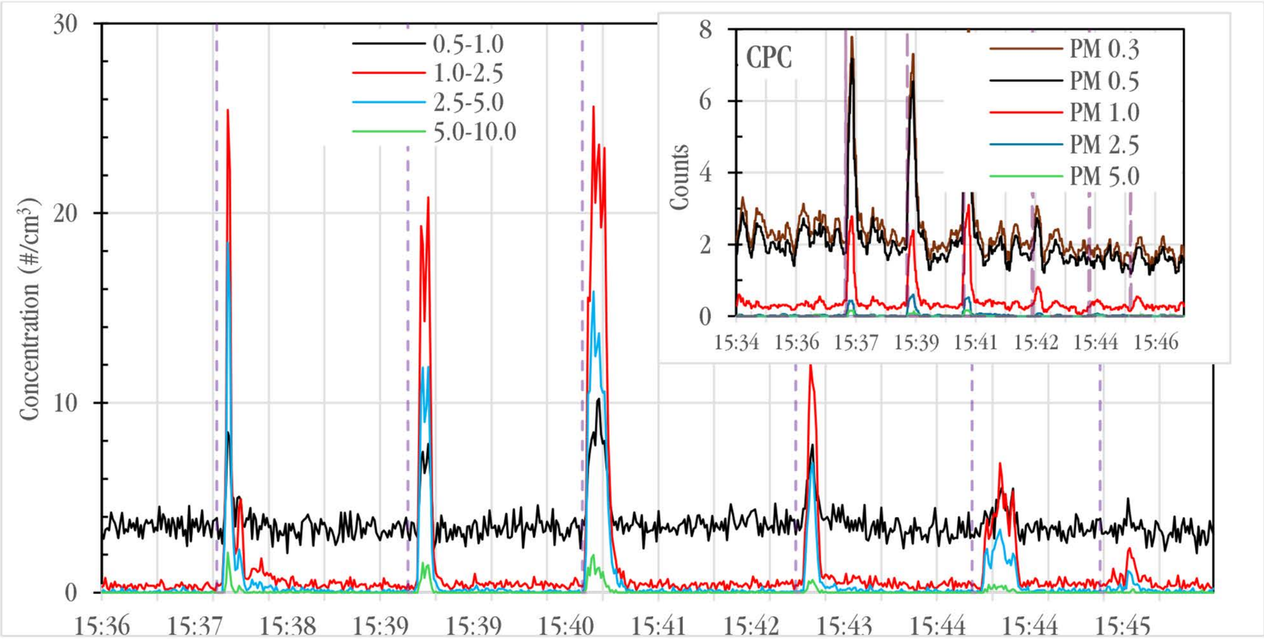

Fig. 7. Collected counts from the APS showing the moment the SUV passed over the test area (vertical, hashed purple lines) coinciding with the strong peaks in air concentration for each size range. Similar responses were collected from the OPC and CPC units (see Supplemental S7, *https://links.lww.com/HP/A354*). The inset graph shows the response of the CPC4, located on the opposite side of the street from the APS unit, indicating that particles smaller than PM1.0 were also resuspended by the vehicle.

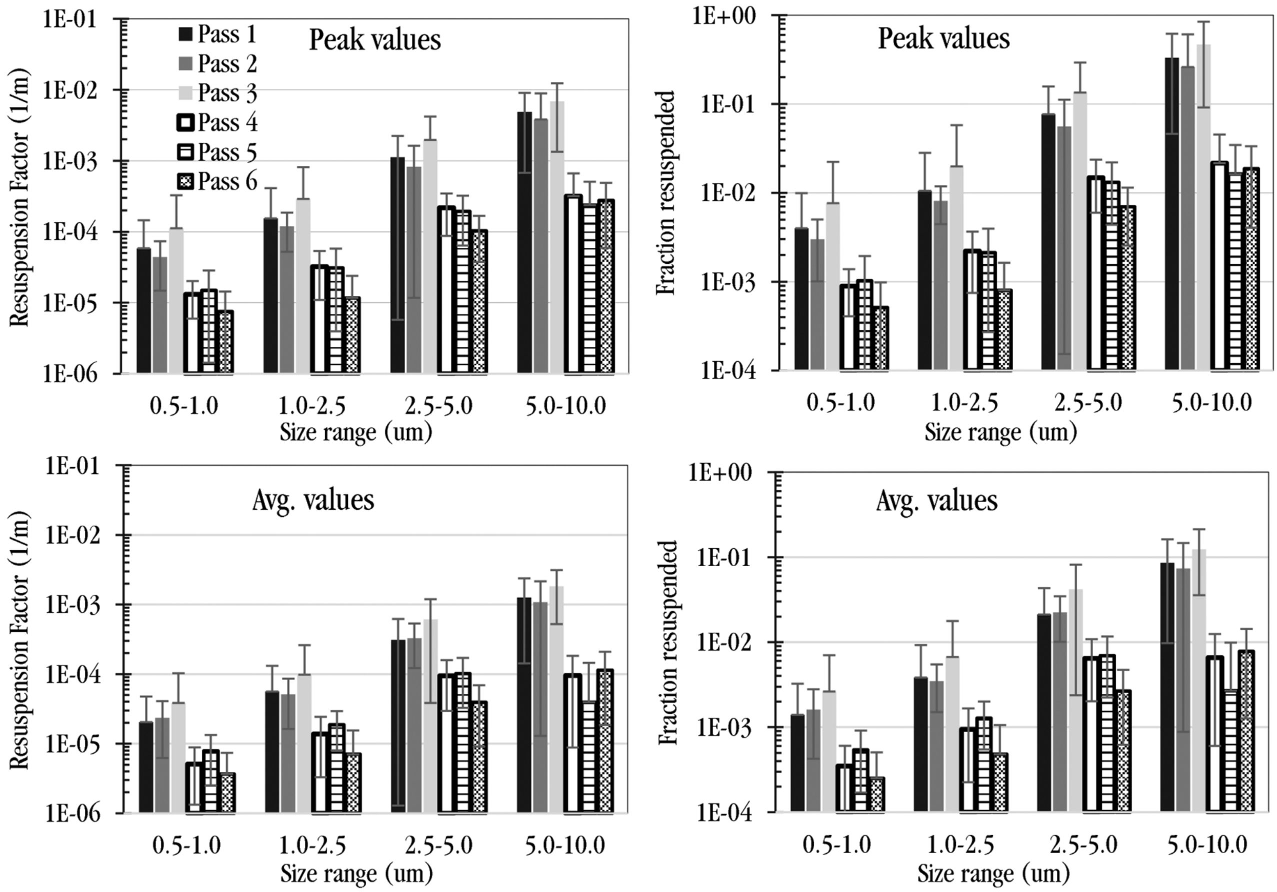

Fig. 8. Peak (top) and average (bottom) resuspension factors (left) and fraction of dust resuspended (right) measured for each of six passes of the SUV through the ATD at 64 km h^{-1} (40 mph).

μm (nominal) CeO_2 particles on concrete pavers at 0.33 m height and S_f orders of magnitude less at respiratory heights of 1.7 m. However, those tests used an electric golf cart at 3-5 mph, which is expected to produce significantly different turbulent wake patterns than a full sized vehicle.

Extrapolation of results. It is important to consider the experimental setups in prior studies and the present study in an attempt to extrapolate to realistic conditions immediately following a deposition of fallout. Nicholson and Branson (1990) used a small test patch, and we reproduced such a scheme in our experiments. This produced an air concentration of particles reflecting the action of the vehicle tires traveling directly over the dust or the vehicle undercarriage traveling over the dust. The data reported is in terms of fraction of dust removed from the pavement from which we can calculate a resuspension factor under those conditions.

However, it is necessary to calculate the equivalent resuspension factors from our experiments to reflect contamination on the entire roadway and subsequent air concentrations and compare to the results of Nicholson et al. and Sehmel. Our experiments and those of Nicholson et al. (1989); Nicholson and Branson (1990) N establish that the amount of dust removed from the roadway with a pass of the vehicle regardless of whether the vehicle tires pass over the dust or the undercarriage passes over the dust is nearly identical. Sehmel established (1973) that particles in adjacent lanes on the road are much less resuspended (order of magnitude less) so will be ignored in this analysis. The air concentrations used to calculate resuspension factors in the present study originate from dust only on a small patch of 0.6 m^2, recognizing that the effective area changes with each pass due to redeposited dust, as mentioned in the **Vehicle drive-through tests** section. However, a SUV covers a footprint of 10 m^2 (1.9 m wide and 5.3 m long). Therefore, the calculated air concentration from the passage of a SUV over a roadway contaminated with dust will be (10 m^2/0.6 m^2) = 16.9 times larger than measured in our experiments. The ground concentration (in g m^{-2}) is unchanged. Thus, the resuspension factor will be 16.7 times larger than what was measured experimentally using our small test patch. Thus, average resuspension factors adjusted for a fully covered, contaminated roadway may be quite large (Table 5). These values are

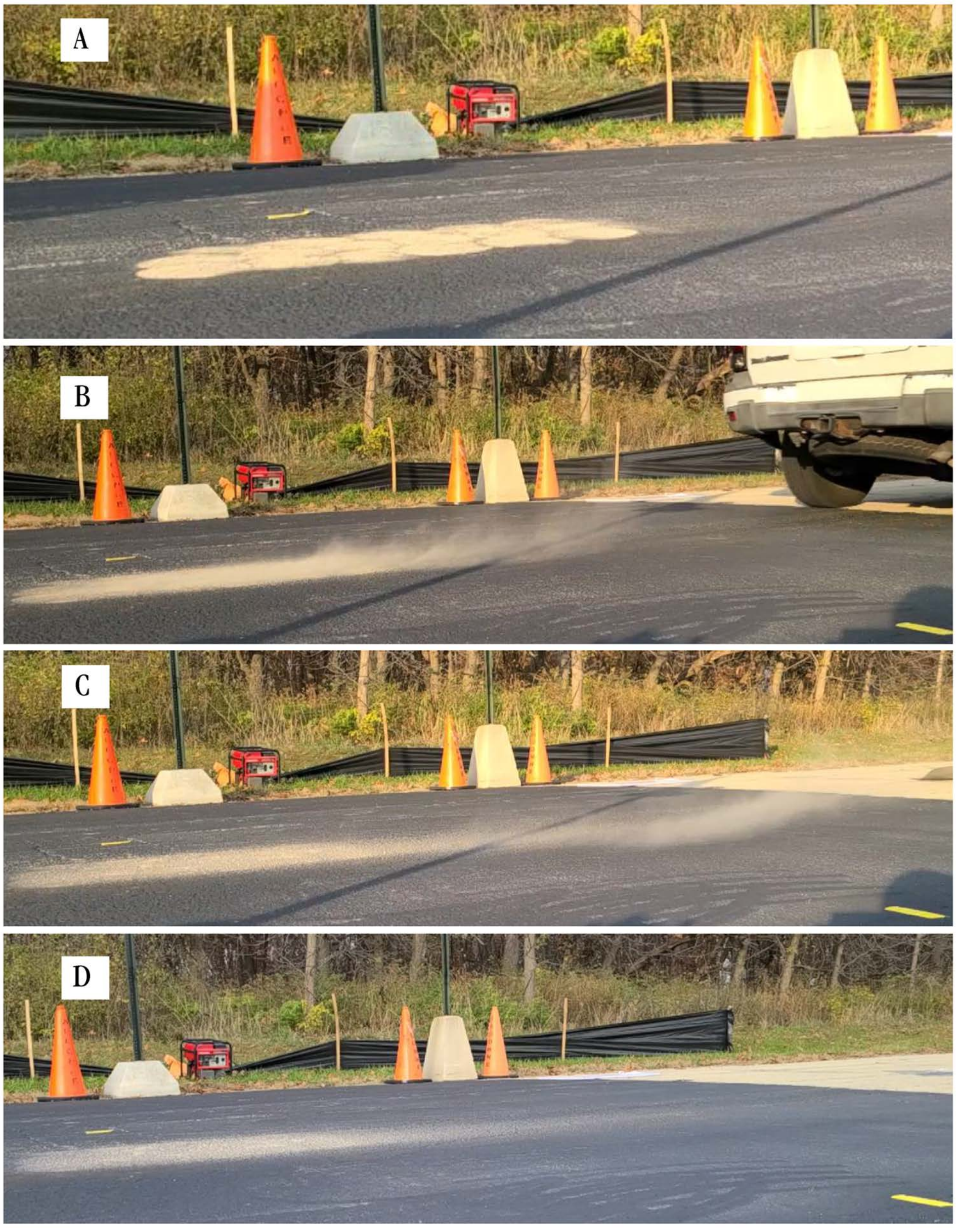

Fig. 9. Photos showing the (A) initial seeding of Arizona Test Dust on the pavement, and successive images (B, C, D) immediately after the SUV passes over the first time.

still within the range calculated from the data of Sehmel and Nicholson (see Supplemental S8, *https://links.lww.com/HP/A354*).

A criticism of our experiments is the high dust loading of particles on the ground, being above a monolayer and thus appreciative particle-particle interactions is expected as opposed to the stronger particle-ground forces to counter uplift of particles due to the tire or turbulence of the air draft. However, the agreement of our data to the results of Sehmel and Nicholson et al., both of whom used much lower dust loading, would suggest that the particle-particle effect may not be as important.

Recommendations

Given the data reported here, we recommended resuspension factors for the following conditions in the emergency phase immediately after release of radioactive material (Table 6). Vigorous pedestrian or personnel movement (marching) data span the values of the average and peak values reported in Table 4 for each size range. Resuspension factors for vacuuming are consistent with

Fig. 10. Side-by-side images of the original seeding of the ground and the residual dust after four drive-over passes.

Table 5. Comparison between S_f (m^{-1}) directly measured in the present study and S_f adjusted for a fully contaminated roadway (estimated uncertainties are ± a factor of 5).

	Pass 1		Pass 6	
Size (µm)	Measured S_f	Adjusted S_f	Measured S_f	Adjusted S_f
0.5-1.0	2×10^{-5}	3×10^{-4}	4×10^{-6}	6×10^{-5}
1.0-2.5	6×10^{-5}	9×10^{-4}	7×10^{-6}	1×10^{-4}
2.5-5.0	3×10^{-4}	5×10^{-3}	4×10^{-5}	7×10^{-4}
5.0-10.0	1×10^{-3}	2×10^{-2}	1×10^{-4}	2×10^{-3}

Table 6. Recommended resuspension factor S_f (m^{-1}). The recommended value for casual walking is the default value provided by the particular model (10^{-6}-10^{-5} m^{-1}).

		Condition					
Particle size (µm)	Vigorous pedestrian or personnel movement	Vacuuming	SUV (64 km h^{-1})	SUV (48 km h^{-1})	SUV (32 km h^{-1})	SUV (16 km h^{-1})	SUV (8 km h^{-1})
0.5-1.0	$2\text{-}6\times10^{-5}$	$1\text{-}5\times10^{-5}$	$0.6\text{-}3\times10^{-4}$	$0.5\text{-}2\times10^{-4}$	$0.3\text{-}1\times10^{-4}$	$0.2\text{-}0.9\times10^{-4}$	$0.1\text{-}0.5\times10^{-4}$
1.0-2.5	$0.9\text{-}2\times10^{-4}$	$1\text{-}5\times10^{-5}$	$1\text{-}9\times10^{-4}$	$0.8\text{-}7\times10^{-4}$	$0.5\text{-}4\times10^{-4}$	$0.3\text{-}3\times10^{-4}$	$0.2\text{-}2\times10^{-4}$
2.5-5.0	$0.7\text{-}2\times10^{-3}$	$1\text{-}5\times10^{-5}$	$0.7\text{-}5\times10^{-3}$	$0.5\text{-}4\times10^{-3}$	$0.3\text{-}2\times10^{-3}$	$0.2\text{-}1\times10^{-3}$	$0.1\text{-}0.9\times10^{-3}$
5.0-10	$2\text{-}6\times10^{-3}$	$1\text{-}5\times10^{-5}$	$0.2\text{-}2\times10^{-2}$	$0.2\text{-}2\times10^{-2}$	$0.1\text{-}1\times10^{-2}$	$0.06\text{-}0.6\times10^{-2}$	$0.04\text{-}0.4\times10^{-2}$

our only measurable value from experiment and those reported in the literature for larger particle sizes that were outside of our limits of detection.

For vehicle experiments, we have several lines of evidence that support the values recommended in Table 6. Both Nicholson studies only reported particles remaining on the ground and thus may be overly conservative when the calculated resuspension factors are reported (Kaminski et al. 2024). Sehmel's experiments report air concentrations and, thus, reflect true resuspension better than Nicholson's data. However, Sehmel used much denser particles that would be more difficult to resuspend than road dust or radioactivity attached to fallout. Our data falls between that of Sehmel and Nicholson and Branson (1990). and thus appears most appropriate. Therefore, resuspension factors for an SUV at 64 km h^{-1} are taken as the adjusted range from the first pass and the sixth pass from Table 5.

To obtain values for speeds <64 km h^{-1}, we point to the data agreement of both Sehmel and Nicholson and Branson (1990). Sehmel reported a range of a factor of 2.75 for resuspension rates between 80 (1×10^{-3} m^{-1}) and 8 km/h (2.75×10^{-3} m^{-1}) for a truck. Nicholson and Branson (1990) resuspension factors are higher (see Table S9) for a medium sized car at 8 (5.5×10^{-2} m^{-1}) and 64 km/h (3.1×10^{-1} m^{-1}), but the relative range of values is similar to Sehmel — a factor of 5.6 difference from highest and lowest speeds. Recognizing the agreement between both prior studies, we will use the ratios from Nicholson's experiments because he explicitly produced measurements at more incremental speeds than Sehmel. The ratio of resuspension factors from Nicholson and

Table 7. Ratio of S_f at speed to S_f at 64 km h^{-1} used to compute S_f at speeds <64 km h^{-1} in Table 6.

Vehicle speed (km h^{-1})	S_f (speed)/S_f (64 km h^{-1})
5	5.6
10	3.4
20	2.1
30	1.3
40	1.0

Branson (1990) is in Table 7 and was used to compute recommended S_f for slower speeds in Table 6.

CONCLUSION

This study provides critical data on resuspension factors (S_f) for pedestrian and vehicle activities on freshly contaminated paved surfaces, addressing a significant gap in the understanding of resuspension dynamics during the emergency phase of a contamination event. Our results demonstrate that resuspension factors during emergency operations can be orders of magnitude higher than the default values (10^{-6} to 10^{-5} m^{-1}) commonly provided to users of current risk assessment models. These findings have important implications for accurately assessing the risks posed by radiological, chemical, and biological threat agents.

Our experiments revealed that casual walking produced low resuspension factors (S_f<10^{-5} m^{-1}), consistent with prior studies. However, vigorous pedestrian or personnel movement (marching) consistent with evacuation scenarios, significantly increased resuspension, with S_f values ranging from 6×10^{-5} m^{-1} for 0.1–1 µm particles to 6×10^{-3} m^{-1} for 5–10 µm particles. Vacuuming activities suspended smaller particles ($S_f = 1.4 \times 10^{-5}$ m^{-1}), while larger particles remained below detection limits. Vehicle tests showed that driving a SUV over contaminated pavement produced substantial resuspension, with S_f values increasing with particle size. Driving the vehicle tires over the contamination or passing the undercarriage over the contamination produced qualitatively similar results. For the first vehicle pass, S_f ranged from 0.6×10^{-4} m^{-1} for 0.5–1 µm particles to 2×10^{-2} m^{-1} for 5–10 µm particles. Subsequent passes reduced resuspension factors by an order of magnitude, but they remained significantly higher than default model values.

These findings underscore the importance of incorporating activity-specific resuspension factors into risk assessment models to improve the accuracy of exposure estimates during emergency response scenarios. The results are particularly relevant for radiological fallout but are also applicable to chemical and biological threat agents, as these contaminants often adhere to environmental dust particles with similar physical properties. By providing more realistic resuspension factors, this study enables modelers to better predict airborne concentrations of hazardous particles, inform decisions on personal protective equipment requirements, and optimize emergency response strategies, such as evacuation vs. shelter-in-place protocols.

While this study provides valuable insights, it also highlights the need for further research. The high dust loading used in our experiments may have increased particle-particle interactions, potentially overestimating resuspension compared to real-world fallout conditions. Additionally, our vehicle tests were limited to a single speed (64 km h^{-1}), whereas slower speeds are more common during emergency operations. Future studies should explore a broader range of dust loadings, vehicle speeds, and environmental conditions to refine resuspension factor estimates further.

Despite these limitations, this work represents a significant step forward in understanding resuspension dynamics during the emergency phase of contamination events. The recommended resuspension factors provided here offer an immediate resource for modelers and emergency planners, enabling more effective mitigation of risks associated with radiological, chemical, and biological threat agents.

Acknowledgments — The research in this presentation was partially funded by the US Department of Homeland Security (DHS) Science and Technology Directorate (S&T) under IAA 70RSAT23KPM000059. Any opinions contained herein are those of the author and do not necessarily reflect those of DHS S&T. This document was reviewed in accordance with DHS policy prior to publication. Note that approval for publication does not signify that the contents necessarily reflect the views of the Agency. Mention of trade names or commercial products does not constitute endorsement or recommendation for use of a specific product.

REFERENCES

Brunskill RT. The relationship between surface and airborne contamination, In: Fish BR, ed. Surface contamination, proceedings of symposium. Oxford: Pergamon Press; 1967: 93–105.

Buttner MP, Cruz-Perez P, Stetzenbach LD, Garrett PJ, Luedtke AE. Measurement of airborne fungal spore dispersal from three types of flooring materials. Aerobiologia 18:1-11; 2002.

Corsi RL, Siegel JA, Chiang C. Particle resuspension during the use of vacuum cleaners on residential carpet. J Occup Environ Hyg 5:232-238; 2008.

Crocker GR, O'Connor JD, Freiling EC. Physical and radiochemical properties of fallout particles. Health Phys 12:1099-1104; 1966.

Ferro AR, Kopperud RJ, Hildemann LM. Source strengths for indoor human activities that resuspend particulate matter. Environ Sci Technol 38:1759-1764; 2004.

Glasstone S, Philips DJ, eds. The effects of nuclear weapons. Washington, DC: US Government Publishing Office; 1977.

Glen A, Pennington HM. Surrogate suspension-resuspension study. Albuquerque, NM: Sandia National Lab; SAND-2020-4899; 2020.

Hambraeus A, Bengtsson S, Laurell G. Bacterial contamination in a modern operating suite. 3. Importance of floor contamination as a source of airborne bacteria. J Hygiene 80:169-174; 1978.

Harper FT, Musolino SV, Wente WB. Realistic radiological dispersal device hazard boundaries and ramifications for early consequence management decisions. Health Phys 93:1-16; 2007.

Ji JH. Size distributions of suspended fine particles during the cleaning of an office. Aerosol Air Qual Res 20:53-60; 2020.

Jones IS, Pond SF. Some experiments to determine the resuspension factor of plutonium from various surfaces, In: Fish BR, ed. Surface contamination. In: Proceedings of Symposium. Oxford: Pergamon Press; 1967: 83–92.

Kaminski MD, Daiyega N, Magnuson M. A review of the resuspension of radioactively contaminated particles by vehicle and pedestrian traffic — Current theory, practice, gaps, and needs. Health Phys 126:216-240; 2024.

Lai AC, Tian Y, Tsoi JY, Ferro AR. Experimental study of the effect of shoes on particle resuspension from indoor flooring materials. Build Environ 118:251-258; 2017.

Lewis RD, Ong KH, Emo B, Kennedy J, Kesavan J, Elliot M. Resuspension of house dust and allergens during walking and vacuum cleaning. J Occup Environ Hyg 15:235-245; 2018.

Nicholson KW, Branson JR, Giess P, Cannell RJ. The effects of vehicle activity on particle resuspension. J Aerosol Sci 20:1425-1428; 1989.

Nicholson KW, Branson JR. Factors affecting resuspension by road traffic. Sci Total Environ 93:349-358; 1990.

Nielsen EC, Fournier SD. FRMAC Laboratory Analysis Manual Volume 1, Revision 0. Albuquerque, NM: Sandia National Laboratories; 2025.

Owens PN, Walling DE. Spatial variability of caesium-137 inventories at reference sites: an example from two contrasting sites in England and Zimbabwe. Appl Radiat Isot 47:699-707; 1996.

Pires do Rio MA, Amarai ECS, Paretzke HG. The resuspension and redeposition of ^{137}Cs in an urban area: the experience after the Goiania accident. J Aerosol Sci 25:821-831; 1994.

Sehmel GA. Particle resuspension from an asphalt road caused by car and truck traffic. Atmospheric Environment (1967) 7:291-309; 1973.

Shaughnessy R, Vu H. Particle loadings and resuspension related to floor coverings in chamber and in occupied school environments. Atmos Environ 55:515-524; 2012.

Tang P, Kita K, Igarashi Y, Satou Y, Hatanaka K, Adachi K, Kinase T, Ninomiya K, Shinohara A. Atmospheric resuspension of insoluble radioactive cesium-bearing particles found in the difficult-to-return area in Fukushima. Prog Earth Planet Sci 9:17:1-15; 2022.

Thorpe A, Harrison RM. Sources and properties of non-exhaust particulate matter from road traffic: a review. Sci Total Environ 400:270-282; 2008.

US Environmental Protection Agency. PAG manual: protective action guides and planning guidance for radiological incidents. Washington, DC: Office of Radiation and Indoor Air Radiation Protection Division, US Environmental Protection Agency; EPA-400/R-17/001; 2017.

■■